SYNTHESIS REPORT
FOR PUBLICATION

CONTRACT N“: BREU 0438

PROJECT N“: BE-4020

TITLE: DEVELOPMENT OF CVD, METALORGANIC PRECURSORS AND PATTERNING TECHNIQUES FOR HIGH Tc APPLICATIONS

PROJECT
COORDINATOR: THE ASSOCIATED OCTEL Co. Ltd., UK

PARTNERS: AIXTRON Semiconductor Technologies GmbH, D

NKT RESEARCH CENTER, DK

TNO-TPD, NL

UNIVERSITY OF STRATHCLYDE, UK

REFERENCE PERIOD FROM: 1.9.91 to 30.11.95
STARTING DATE: 1.9.91 DURATION: 51 MONTHS

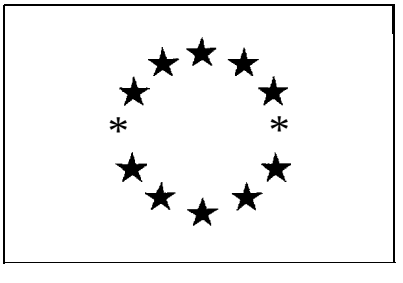

PROJECT FUNDED BY THE EUROPEAN COMMUNITY UNDER THE BRITE/EURAM PROGRAMME

DATE: 30.11.95

DEVELOPMENT OF CVD, METAL-ORGANIC PRECURSORS AND PATTERNING TECHNIQUES FOR HIGH TC APPLICATIONS

B.C. Richards[a], S.L. Cook[a], D.L. Pinch[a], G.W. Andrews[a], G. Lengeling[b], B. Schulte[b], Y.Q. Shen[c], P. Vase[c], T. Freltoft[c], C. I.M.A. Speed, K. Timmer[d], J.L. Linden[d], M.L. Hitchman[e], S.H. Shamlian[e].

[a] *The Associated Octel Co. Ltd., PO Box 17, Oil Sites Road, Ellesmere Port, L654HF, UK.*
[b] *AIXTRON GmbH, Kackertstrasse 15- I 7, D-52072 Aachen, Germany.*
[c] *NKT Research Center, Sognevej 11, DK-2605, Brøndby, Denmark.*
[d] *TNO-TPD, PO Box 595, 5600 AN Eindhoven, The Netherlands.*
[e] *University of Strathclyde, Department of Pure and Applied Chemistry, 295 Cathedral Street, Glasgow, G1 1XL, UK.*

Abstract

MOCVD of superconducting $YBa_2Cu_3O_{7-\delta}$ thin films using the novel precursors $[Y(TMHD)_3.4^tBuPyNO]$[1], $[Ba(TDFND)_2.tetraglyme]$[2] and $[Cu(TDFND)_2]$ and the traditional precursors $[Y(TMHD)_3]$ and $[Cu(TMHD)_2]$ are reported. The novel complexes are low melting (100, 72 and 68 "C respectively), are thermally stable to 200 "C and allow reproducible and reliable film deposition even when maintained at elevated temperatures for several weeks. Conversion of the fluoride to the oxide is achieved by *in situ* hydrolysis.

Films deposited on $SrTiO_3$(100) were shown to be homogeneous layers of $YBa_2Cu_3O_{7-\delta}$, **-0.25** μm thick. The films were epitaxial with good c axis orientation. Critical temperatures, T_c, were typically 91 K and critical current densities, J_c (at 77 K), -5 MA cm^{-2} are achieved. SIMS results showed levels of residual fluorine as low as 10^{-4} F atoms per YBCO.

Highly oriented $SrTiO_3$ has been deposited by MOCVD onto Si, MgO and laser ablated YBCO(PLD) using the novel precursor $[Sr(HFA)_2.tetraglyme]$[3]. An YBCO(PLD)/$SrTiO_3$(MOCVD)/YBCO(PLD) multilayer was constructed. The top YBCO layer possessed a T_c of 89 K and J_c of 2.7 MA/cm^2 at 77K.

In situ studies by FTIR and mass spectroscopy of the variation of the decomposition characteristics as a function of temperature for some of the complexes, as shown by changes in the absorption coefficients, have been related to the molecular structures.

1 Introduction

Metal Organic Chemical Vapour Deposition (MOCVD) has been extensively investigated for the deposition of high temperature superconducting thin films for several reasons [1 -3]. For example, it has the ability to cover large surface areas uniformly at high deposition rates and

---

1 TMHD = 2,2,6,6 -tetramethylheptane-3,5 -dionate
4-^{t}BuPyNO = para *tert*-butyl pyridine N oxide
2 TDFND = 1,1,1,2,2,3,3,7,7,8,8,9,9,-,9-tetradecafluorononane-4,6-dionate
tetraglyme = 2,5,8,11, 14-pentaoxapentadecane
3 HFA = 1,1, 1,5,5,5 -hexafluoropentane-2,4 -dionate

high concentrations of oxygen. It is also possible to grow single phase systems and control the stoichiometry, crystal structure, film morphology and orientation of the Iayers.

To complement the technique, precursors are required that possess high vapour pressure and good thermal stability. Typical precursors for the deposition of the mixed metal oxide $YBa_2Cu_3O_{7-\delta}$ are metal complexes of the ß-diketonate, 2,2,6,6-tetramethylheptane-3 ,5-dione (TMHD). TMHD comprises pentane-2,4-dione (ACAC) with bulky tertiary butyl substituents which are required to shield the metal ions from the intermolecular forces which would otherwise render the complexes involatile. The ligand is suitable in the case of Y and Cu because $[Y(TMHD)_3]$ and $[Cu(TMHD)_2]$ sublime readily and reproducibly between 100 and 150 'C. The shielding effect of the bulky substituents is insufficient, however, for Ba and oligomerisation occurs yielding the tetramer $[Ba(TMHD)_2]_4$ [4]. As a result, the material is significantly less volatile and requires heating to much higher temperatures, 200-250 "C, before evaporation occurs, In addition, the material has been found to decompose at elevated temperatures [5]. Efforts to improve the volatility of $[Ba(TMHD)_2]_4$ have used high purity complexes and restricted the time they are subjected to the elevated temperatures [6] or added a suitable ligand material, such as THF or H(TMHD), to the carrier gas stream [7].

An alternative approach is to employ fluorinated β-diketones. The replacement of hydrocarbon with perfluorocarbon substituents provides good steric hindrance without significant formula weight increase. The possibilities for intra-molecular hydrogen bonding are reduced and van der Waals interactions appear to be lower. Comparison of the thermal properties of $[Ba(TDFND)_2.H_2O]_n$ with the non-fluorinated $[Ba(TMHD)_2]_4$ showed the former to be more volatile [8]. Following loss of water, it evaporates at atmospheric pressure without decomposition. Previously reported varying CVD deposition rates obtained when using the new anhydrous form of the precursor $[Ba(TDFND)_2]$ have been investigated [9] using a range of techniques for analysing hydrated and anhydrous forms of the precursor before and after use for deposition. It has been shown that, apart from water loss from the hydrate, there are no significant molecular structural changes to the precursor in use. X-ray powder diffractograms show that there is the possibility of crystalline growth. A simple model of spherical crystallite coalescing has been considered and it has been shown that the range of behaviour observed in practice with solid precursors can be satisfactorily explained by the model. When full cognizance is taken of the effects of precursor purity and degree of crystallinity it is found to be possible to grow reproducibly high quality BaF_2 and superconducting YBCO. The precursor $[Ba(TDFND)_2]$ is thus a potentially useful new material for MOCVD of YBCO and other barium containing films.

An alternative strategy to overcoming any problems associated with solid precursors is to prepare precursors which are molten at the temperature of use. Formation of Lewis base adducts is known to lower the melting point of β-diketonate complexes. The use of polydentate Lewis base ligands has been shown to provide adducts which are sufficiently stable towards dissociation and decomposition that they can be used for CVD purposes [10]. The combination of $[Ba(TDFND)_2]$ with the polyether, tetraglyme, is particularly advantageous because of its low melting point (70-72 'C) and ability to volatilise intact at ambient pressure [11]. The complex, $[Ba(TDFND)_2.tetraglyme]$, is stable to -300 "C. An analysis of the X-ray crystal structure and molecular structure of the complex has shown [12] that the barium atom is nine co-ordinate with binding to all the O atoms. The two BaTDFND rings are planar but tilted by 26° from being coplanar. The 5 0 atoms of the tetraglyme

ligand are also essentially coplanar but this plane subtends angles of 88.8(1)0 and 67.4(1)0 to the two BaTDFND planes. The Ba-O (TDFND) bond lengths are longer than for other related compounds but the Ba-O (tetraglyme) bond lengths are similar to those in [$Ba(HFA)_2$.tetraglyme]. The low melting point and the fact that [$Ba(TDFND)_2$.tetraglyme], alone of barium complexes of this kind, can be evaporated without decomposition at 1 atm are attributed to lower intermolecular forces for this compound and to its greater thermal stability.

Thermal decomposition of fluorinated Ba precursors in an anhydrous atmosphere yields BaF_2 in preference to BaO. A study by FTIR spectroscopy of the gas phase thermal decomposition of [$Ba(TDFND)_2$.tetraglyme] under a total pressure of 10 torr for a temperature range 200-650°C in the absence and presence of oxygen has been made [13]. Once formed the fluorine in the layer can be removed by hydrolysis in a post deposition treatment at elevated temperatures. Films deposited by this method have been found to be non epitaxial and possess inhomogeneous surface morphology [14] . However, if water is introduced into the gas phase mixture during the deposition process, the Ba precursor will be hydrolyses to the oxide. Watson et al. [15] studied the effect of *in situ* water on the growth of superconducting films and reported epitaxial thin films of $YBa_2Cu_3O_{7-\delta}$ with -excellent superconducting properties: critical temperature, T_c = 91.8 K and critical current density, J_c = 1.5 MA cm^{-2} at 77K. Using light element electron probe micro analysis, EPMA, they were unable to detect the presence of residual fluorine in the films. However, for elements with atomic number less than 10, a detection limit of only 1000 ppm (O. 1%) is typical for this method [1 6].

We have previously reported the formation of superconducting $YBa_2Cu_3O_{7-\delta}$ on MgO by MOCVD using the novel Ba precursor [$Ba(TDFND)_2$.tetraglyme] [1 1]. This was the first time a liquid Ba precursor that is stable at atmospheric pressure had been used. The initial films consisted of a mixture of Y and Cu oxides and BaF_2. Conversion to the superconducting oxide was effected by post deposition annealing with water and oxygen. In this paper we report the successful deposition of good quality $YBa_2Cu_3O_{7-\delta}$ films produced by *in situ* MOCVD using [$Ba(TDFND)_2$.tetraglyme]. The *in situ* process enables epitaxial films to be grown and eliminates the need for a post annealing step. [$Ba(TDFND)_2$.tetraglyme] is a thermally stable precursor and is used at temperatures above its melting point but significantly below that required for other non-fluorinated materials. The versatile MOCVD system employed enables precise control of the temperature, pressure and carrier gas flow for each individual precursor, including water, leading to homogeneous and reproducible films. A detailed investigation of the stoichiometry, surface morphology, epitaxy, superconducting transition temperature and critical current density has been made. Special attention has been paid to examining the fluorine content of the films using Secondary Ion Mass Spectrometry (SIMS) for which a detection limit better than 20 ppb can be achieved.

With the successful introduction of the very stable and at the same time liquid Ba precursor, the stability of the Y precursor and the limited reproducible evaporation from the solid Y and Cu precursors became the limiting factor in obtaining reproducible introduction of precursors into the reactor. We report the synthesis of the complexes [$Y(TMHD)_3$.4^{t}BuPyNO] and [$Cu(TDFND)_2$] which melt at 100 and 68 “C respectively. High quality YBCO films have been reported using the 3 liquid precursors [17].

Due to the relatively high YBCO deposition temperature, severe chemical reactions take place between a range of substrate materials and the superconductor. Buffer layers can be used to prevent these chemical reactions and to create better lattice matching. Typical buffer layers include Y_2O_3, yttria stabilised zirconia (YSZ), $SrTiO_3$ and CeO_2. Their insulating properties can also be exploited in the formation of multilayers in which superconducting layers are separated by thin non-conducting layers eg. YBCO/$SrTiO_3$/YBCO. A novel fluorinated Sr precursor, [Sr(HFA)$_2$.tetraglyme] was synthesised and used in the MOCVD of $SrTiO_3$ as a buffer layer on Si and MgO and as an insulating layer between two layers of laser ablated YBCO. The properties of the multi layer are reported,

Although good quality HTS films have been produced by MOCVD, if careful control of the properties and quality of HTS layers grown by this method is to be achieved routinely, then it is essential to try to understand the factors affecting film growth. Little has been reported, however, on the thermal decomposition of any of these compounds, especially in the presence of oxygen which is necessary for the growth of HTS layers. The only studies which have been carried out have been by mass spectroscopy for the thermal decomposition of [Cu(TMHD)$_2$] and [Y(TMHD)$_3$] [18-20]. In situ FTIR spectroscopy is a useful complementary technique since it can probe the decomposition directly in the reactor. and at the same time give information about bonding changes. Also it does not suffer from some of the disadvantages of mass spectroscopy, such as sampling difficulties, disturbance of the species in the gas phase, and blocking of an orifice. Therefore in order to try and obtain a better understanding of the chemical decomposition of [Y(TMHD)$_3$], [Cu(TMHD)$_2$] and [Ba(TDFND)$_2$.tetraglyme], which have been used as precursors for the MOCVD of HTS thin films in this work, we have begun a study by FTIR of their thermal decomposition in the gas phase in the absence and presence of oxygen under typical deposition conditions and we have begun to relate the results to mass spectroscopic investigations carried out in parallel.

2 Technical Description

2.1 *Precursor Synthesis*

[Y(TMHD)$_3$.4-^{t}BuPyNO] [11] was prepared by the dissolution of [Y(TMHD)$_3$] (Lancaster) (0.64 g, 1 mmol) and 4-^{t}BuPyNO (O. 17 g, 1 mmol) in CH_2Cl_2 (15 cm^3). The solution was stirred over $MgSO_4$ for 30 minutes, filtered, then evaporated to dryness before recrystallisation from minimal quantities of hexane. Melting point 10O°C, 'H nmr δ 1.27 (s, 54H, TMHD C$\underline{H}_3$), δ 5.94 (s, H, COC$\underline{H}$CO), δ 0.76 (S, 9H, PyNO C$\underline{H}_3$) and δ 6.46 and 8.17 (d, 2H, PyNO C$\underline{H}$). C/H/N found versus (calculated)% m/m C 63,30 (63.89), H 8.65 (8.87) and N 1.87 (1.78).

The synthesis of the precursor [Ba(TDFND)$_2$.tetraglyme] has been described in detail previously [11, 21]. It is a highly volatile material that shows good thermal stability at atmospheric pressure. Its low melting point, 72 'C, offers the advantage that it is liquid at the temperature of use [11].

Cu(TDFND)$_2$ was prepared by the addition of HTDFND (5.0 cm^3, 10 mmol) to a solution of copper sulphate (1.56 g, 6 mmol) in deionised water at ambient temperature. A green oil immediately separated, became progressively more viscous and after thirty minutes yielded a suspension of bright green solids. The solids were collected by filtration and dried under vacuum over P_2O_5. The resulting dark green solids were found by STA (see section 3.1) to

be the hydrated complex $[Cu(TDFND)_2].H_2O$. The solids were sublimed at 90°C, 0.5 mbar. Grey-green solids were isolated that possessed a melting point of 68°C. Elemental analysis of the sublimed material showed it to be the anhydrous $[Cu(TDFND)_2]$ {C 24.67 (24.62) and H 0.26 (0.23) found versus (calculated)% m/m}.

The synthesis of the precursor [Sr(HFA).tetraglyme] has been described in detail previously [22]. It is a colorless solid material with a melting point of 137- 139°C. The complex rapidly and almost quantitatively sublimes at 115°C/0.01 mm Hg

2.2 *Fundamental Studies*

For the FTIR studies the experimental arrangement consisted of an FTIR spectrometer, a gas-handling facility, a reactor made up of an evaporator, a reactor tube and a thermostatted jacket, and a vacuum system. The FTIR spectrometer was a Mattson Research Series instrument with a EG&G Judson HgCdTe detector (model: J15D14-M1OO7-SO1 M-45-005603). The gases used were nitrogen (BOC, silicon grade) and oxygen (Air Products, 99.6%). The yttrium precursor (Inorgtech, 99.9%) and the copper precursor (Lancaster Synthesis, 99.1 %) were used as supplied without further purification. The barium precursor was provided by Octel and was also used as received. The precursor being studied was heated in a stainless steel evaporator-. The temperature of the precursor was measured by a thermocouple situated on the top surface of the precursor and temperatures of 132°, 117°C and 125°C were used for $[Y(TMHD)_3]$, $[Cu(TMHD)_2]$ and [Ba(TDFND)$_2$.tetraglyme], respectively; these are typical precursor temperatures for deposition of HTS layers [18]. The precursor vapour was carried to the reactor by a constant flow of 100 seem of nitrogen and to prevent condensation of the precursor before it reached the reactor the wall of the jacket was heated to 200°C. For experiments with oxygen a constant flow of 40 seem through a side arm in the evaporator was used.

The reactor was made of quartz and had one inlet and two outlets. The diameter was 2.5 cm and the length was 27 cm. The temperature range investigated in the reaction zone was 200-650°C and the total pressure was 1.33 x 10^3 Pa (10 Torr). The temperature of the decomposition zone was monitored by a thermocouple placed centrally on the outside of the reactor tube, but this temperature was related to the temperature in the centre of the reaction tube by a calibration measurement made beforehand. The pressure was monitored with a Baratron guage positioned in the exhaust line. The windows of the reactor tube were kept free from deposits by flushing with a flow of 80 seem of nitrogen.

Several spectra of the vapour in the decomposition zone were obtained at each temperature for the spectral region extending from 4500 cm-l to 700 cm-l.

As a complementary technique, in situ mass spectroscopic analysis has been attempted. However, a number of serious problems have been encountered. Briefly, these problems were partly associated with contamination of the quadruple, but, more significantly, with condensation of precursors at the inlet of the spectrometer. To try and overcome this latter problem a variety of designs for introducing large molecular weight precursors into the mass spectrometer, together with gas handling arrangements, were investigated. First of all, a heated box at the entrance zone of the spectrometer was constructed to maintain the sampling and analyser heads at above 100”C at all times. This proved to be successful in stopping the condensation of precursors at the inlet of the mass spectrometer which had resulted in the orifice becoming blocked previously. The arrangement was further extended to include a

small reactor and valve switching system, also all heated. The reactor temperature could be varied from 10O°C to greater than 600°C. There were, though, still problems in obtaining signals which corresponded to changing conditions within the reactor, since there were long term memory effects within the system. Finally, after much effort a simplified switching and heating system was designed and built. This appeared to overcome all the major problems previously found.

2.3 *Reactor Design*

In order to grow high quality HTS thin films, an MOCVD system was designed that could control the evaporation of the metal-organic precursors very precisely. This was of particular importance because the equipment was required to evaporate various types of precursor (including solids) each with a different vapour pressure. The inherently low vapour pressures common to the metal-organic precursors for $YBa_2Cu_3O_{7-\delta}$ and other HTS ceramics made it necessary to heat the precursors in order to evaporate them. The MOCVD system was therefore designed to control the temperatures of the precursors to an accuracy of ±0.1°C up to a maximum of 200 “C. A precisely, controlled carrier gas flow was fed through the bubbler containing the heated solid or liquid precursor. To ensure very stable evaporation conditions, the internal pressure in each bubbler was independently controlled by a pressure regulator suitable for operation at the elevated temperatures mentioned. As a consequence, the precursor temperature, the carrier gas flow through the bubbler and the pressure inside the bubbler could be independently controlled. This resulted in highly reproducible evaporation rates.

Nitrogen and oxygen were used as carrier gas and oxidising agent respectively. A continuous flow of water vapour was employed to enable *in situ* removal of fluorine. Rapid switching of the precursors from the bubblers to the reaction chamber was achieved by means of a vent/run manifold. This allowed the addition of a stabilised precursor flow from the vent line, maintained at the same pressure as the reaction chamber, into the run line and vice versa. With gas velocities of 1 -3 m s^{-1}, switching times between vent and run lines of less than 0.1 s were possible. All vent and run lines, including valves and fittings, were held at temperatures slightly higher than those of the bubblers to prevent condensation of precursors on cooler surfaces,

A cold wall, horizontal flow, quartz reaction chamber was employed. The substrates were located on a silicon carbide coated, graphite susceptor with a maximum capacity of one 2 inch diameter substrate. The susceptor was heated by infrared lamps with 6 kW total power allowing susceptor temperatures up to 1000 “C to be achieved. At a later stage of the project a Gas Foil Rotation® Susceptor was introduced to the MOCVD reactor. Using this technique the substrate was rotated using a gas flow only. The advantage is that no feedthroughs are required and no particles are generated by mechanical friction. The rotation of the substrate leads to a strong increase of the homogeneity due to averaging the gas phase depletion which is inherent to MOCVD processes.

The pressure in the reactor was controlled by a closed loop arrangement comprising a capacitive manometer and throttle valve controlling the pumping speed of the rotary vane pump. The vacuum system allowed operation of the reactor from 10-3 mbar (10-1 Pa) to atmospheric pressure.

2.4 *MOCVD of YBCO*

Conditions for the use of the three precursors and water are given in Table 1. The reactor was designed such that two precursors shared each run line in the gas phase en route to the reactor. Water vapour was transported along the same line as $[Cu(TMHD)_2]$ as the latter was synthesised using an aqueous route and was considered least likely to undergo premature hydrolysis or decomposition. Prior to deposition, the precursors were allowed to equilibrate under deposition conditions with all gas phase materials exiting via heated vent lines,

Table 1: MOCVD Parameters for Deposition of $YBa_2Cu_3O_{7-\delta}$ on $SrTiO_3$ (100)

(a) Precursor Conditions

Temperature /°C	Y:	145
	Ba:	145
	Cu:	141
	H_20:	52
Pressure /mbar	50-200	
N, flow rate /seem	50-150	

(b) Reactor Conditions

Susceptor temp /°C	830-880
Estimated substrate temp /°C	800-850
Total flow rate /seem	1720
0_2 partial pressure/ mbar	1.7
Pressure /mbar	10
Deposition time /rein	100

(c) Post Deposition Treatment

Atmosphere	o*
Flow rate /seem	1720
Reactor pressure /mbar	1000
Initial susceptor temp /°C	830-880
Final susceptor temp /°C	300
Cooling rate /°C rei^{n}-'	10-20

The reactor chamber was maintained at a constant pressure of 10 mbar (103 Pa). Depositions were carried out with susceptor temperatures between 830 and 880 *C which corresponded to a substrate temperature approximately 30 'C lower. The substrates were $SrTiO_3$ (100) 8 x 8 x 0.5 mm (Crystal GmbH). The total gas flow through the reactor chamber was 1720 seem. The partial pressure of 0_2 in the reactor was 1.7 mbar (170 Pa). The reaction chamber was left to equilibrate for 20 minutes under deposition conditions prior to introduction of the precursors, At the start of the deposition, the precursors were directed to the reactor chamber simultaneously.

To finish each deposition, the precursor pots were closed but the carrier gases continued to flow through the deposition chamber. After 10 minutes the atmosphere and pressure in the chamber was changed to dry 0_2 (1720 seem) at 1 bar (10^5 Pa). The chamber was cooled to 300 °C at 10 - 20 *C rei^{n}-' and to ambient temperature by self cooling. All films were stored in dry air prior to characterisation.

2,5 *MOCVD of $SrTiO_3$*

A test reactor with a cold wall, stagnation flow, quartz reaction chamber was employed. The Sr precursor [Sr(HFA)$_2$.tetraglyme] and the Ti precursor $[Ti(OPr^i)_4]$ were evaporated using bubbler type evaporators. Nitrogen was used as carrier gas. Oxygen was used as oxidising agent. Although fluorine free Sr- and Ti- oxides could be deposited, the addition of water seemed necessary to obtain single phase $SrTi0_3$. Water was introduced using a Bronkhorst Hi-Tee liquid mass flow controller in combination with a Bronkhorst Hi-Tee controlled evaporator mixing system (CEM). The process cycle for the deposition experiments of $SrTiO_3$ on YBCO started with pumping down of the reactor in a 1:1 N_2:02 atmosphere followed by heating the susceptor to 800°C using a 200 kW RF generator. The deposition is performed using deposition times varying from 30 to 180 minutes. In the final step, the pressure in the reactor is increased to 1 bar (105 Pa) of oxygen and the sample cooled at 5°C/min.

2.6 Film Characterisation

Observations of surface morphology and quantitative analysis were carried out in a Leica Cambridge S360 Scanning Electron Microscope (SEM) fitted with an Energy Dispersive X-ray Spectrometer (EDX) (Oxford Instruments) with conventional ZAF correction software, modified to take account of the thin film sample geometry. The modification allowed the measurement of film thickness and was calibrated to an $YBa_2Cu_3O_{7-\delta}$ film of known composition and depth. An accelerating voltage of 17 kV was used for quantitative analysis.

The films were studied by ac susceptibility at 10 Hz in a standard two coil mutual inductance set-up to determme critical temperature, T_c, and estimate critical current density,. $J_{c\ (inductive)}$. The critical current density, $J_{c\ (transport)}$, was determined by 4 point transport measurement after the film had been patterned.

Crystal structure and crystallographic orientation of the films were characterised by X-ray diffraction (XRD). 2θ scans were measured on a Rigaku diffractometer. Rocking curve analysis was performed using a Hilger and Watts 4-circle diffractometer,

Secondary Ion Mass Spectrometry (SIMS) was carried out on a SIMSLAB quadruple SIMS instrument (Fisons Instruments - Surface Science Division) with a 1-800 amu quadruple mass spectrometer. The depth profiles for fluorine were obtained using 10 keV Ga^+ with a current of 25 nA into an area of approximately 250 x 250 pm. The instrument operated in the negative secondary ion mode at a base pressure less than 10^{-9} mbar (10-7 Pa). A Dektak profilometer was used to characterise the resulting craters.

2.7 Multilayer

A multilayer structure of YBCO (PLD) / $SrTiO_3$ (MOCVD) / YBCO (PLD) has been prepared in order to study the properties of $SrTiO_3$ deposited in the YBCO layer. The bottom YBCO layer was deposited on the $SrTi0_3$ substrate by pulsed laser deposition technique [23]. After the deposition of $SrTiO_3$ by MOCVD, patterning on the $SrTiO_3$ was carried out in order to uncover part of the bottom YBCO layer. The patterning was done by electron beam lithography and Ar ion milling [24]. Finally a top YBCO layer and a Au contact layer were deposited by the PLD technique. The top layers were again patterned by electron beam lithography and Ar ion milling. Two patterns were prepared in this structure. One was for the measurement of the resistance between the top and the bottom layer. The other one was a 3.5 μm wide bridge in the top YBCO layer.

3 **Results**

3.1 *Fundamentals Studies*

Results obtained for [$Cu(TMHD)_2$] showed that the ring structure is less stable than in the case of [$Y(TMHD)_3$]. For [$Ba(TDFND)_2$.tetraglyme] the results were rather more complicated with evidence for the disappearance of the C-F stretch; it is thought that this is because CF_3 breaks off the ring and joins to a barium atom to form $BaF(CF_3)$.

The variation of the decomposition characteristics for the complexes [$Y(TMHD)_3$], [$Cu(TMHD_2$] and [$Ba(TDFND)_2$.tetraglyme] as a function of temperature have been related

to their molecular structures. This can be illustrated by reference to the decomposition of $[Y(TMHD)_3]$. A typical spectrum for $[Y(TMHD)_3]$ at 200°C is shown in Figure 1; it is interesting to note the sensitivity y of the FTIR instrument of about 0.010/O. Characteristic spectral bands for $[Y(TMHD)_3]$ at 200°C appear at 2967 cm^{-1} which can be suggested to be due to the $C\text{-}H_x$ stretch of the tertiary butyl groups, at 1571-1556 cm-* arising from C=C or C=O stretching in the rings, and at 1508 cm-' and 1408 cm^{-1} also due to ring C=C stretching. The absorption coefficient (α) was calculated from the relation $\alpha = [\ln(I_0/I]/d$ where I_0 is the background intensity, I the peak intensity and d the length of the tube between the two NaCl windows. Values of the absorption coefficient normalised to the corresponding mean value obtained at 200°C are plotted as a function of temperature in Figure 2.

Up to about 400°C and in the absence of oxygen the slight decrease of the relative absorption coefficient with temperature observed (Figure 2(a)) is similar for the absorption due to vibrations from both the ring and the ring substituents, Bu^t. This variation mainly reflects the inverse dependence of the concentration of a gas on temperature at constant total pressure. In the region 400-450"C the absorption arising from the C=C and C=O stretches begins to decrease slightly more rapidly than the absorption attributed to the C-H stretch. This suggests that the structure of the rings is less stable than the hydrocarbon moiety. The stability of the C-H bonds is not surprising since it is well known that thermal cracking of such bonds requires considerably higher temperatures than those used here. The appearance of a small peak at 2157 cm^{-1} indicating the formation of CO at temperatures above ca. 525°C is consistent with the breakup of the rings. Also this is not too unexpected if one compares the Y-O bond length of 0.227 nm with the value of 0.230 nrn expected on the basis of the appropriate ionic radii; there clearly is not a strong orbital overlap and shortening and strengthening of the bond.

In the presence of oxygen, again up to about 400°C a similar variation of absorption coefficient with temperature is observed for all the four main bands (Figure 2(b)). Above ca. 400°C there is a much more dramatic increase in the relative absorption coefficient with temperature and above ca.570°C none of the four initial vibrational modes can be detected. The appearance of a peak in the spectrum at 2367 cm-' due to CO_2 for temperatures> 450°C, and reaching a constant value for temperatures greater than about 500°C, shows that oxidation of the entire organic structure is occurring, although again the hydrocarbon moiety seems to be slightly more resistant to decomposition than the rings.

The FTIR results presented here are in reasonable accord with the mass spectroscopic results. These show that in the absence of oxygen the precursor began to decompose at about 500°C, which is only slightly higher than the region of 400-450°C where we observe the ring structures starting to break up. They also show CO beginning to appear at ca. 550°C, which is close to the temperature of 525°C mentioned above. In the presence of oxygen, mass spectroscopy shows decomposition starting at about 400°C with practically no precursor signals left by ca. 600°C and with significant amounts of $C0_2$ being detected for temperatures of >400°C. All these observations are **in** general agreement with those made here, with the FTIR results having the potential for yielding more information about the chemical changes occurring during the decomposition of the precursors.

As a result of the experimental developments mentioned above we have now been able to obtain with mass spectroscopy a variation of the decomposition of yttrium and copper

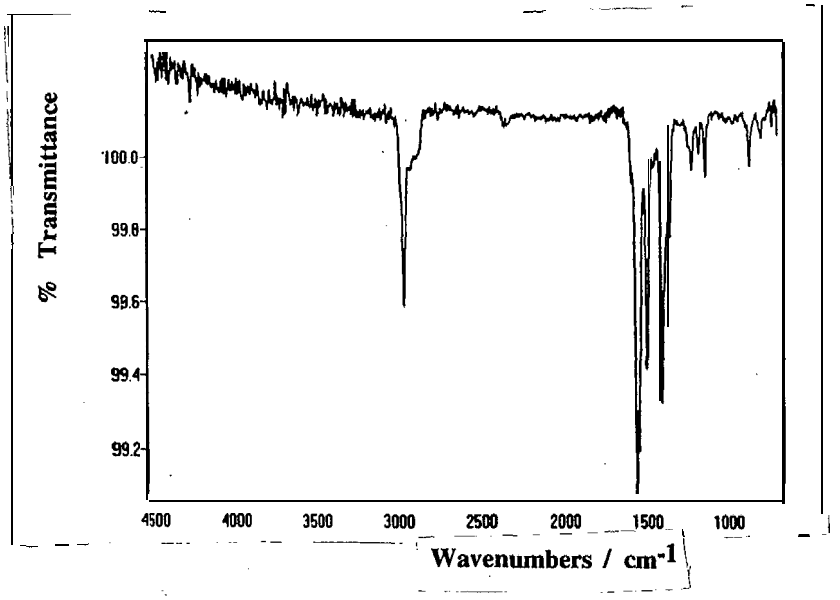

Figure 1: Typical FTIR spectrum of $[Y(TMHD)_3]$

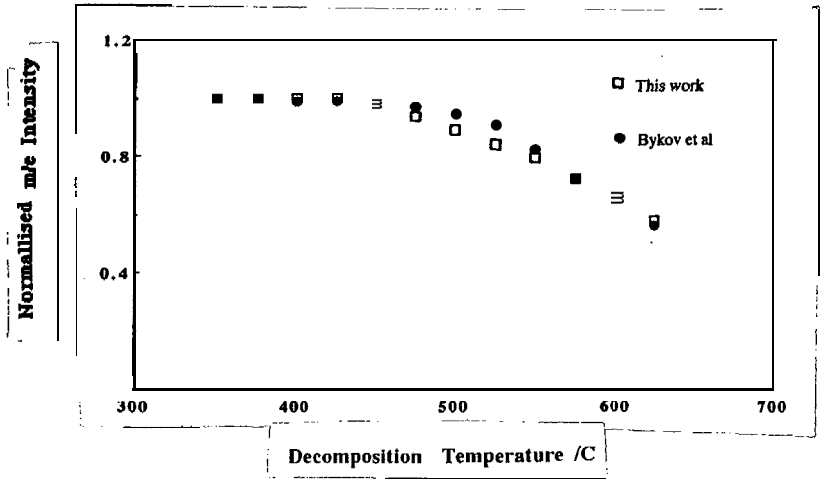

Figure 3: The relationship between $[Y(TMHD)_3]$ molecular ion intensity as detected by MS and its decomposition temperature. A comparison of our results with those of Bykov et al.

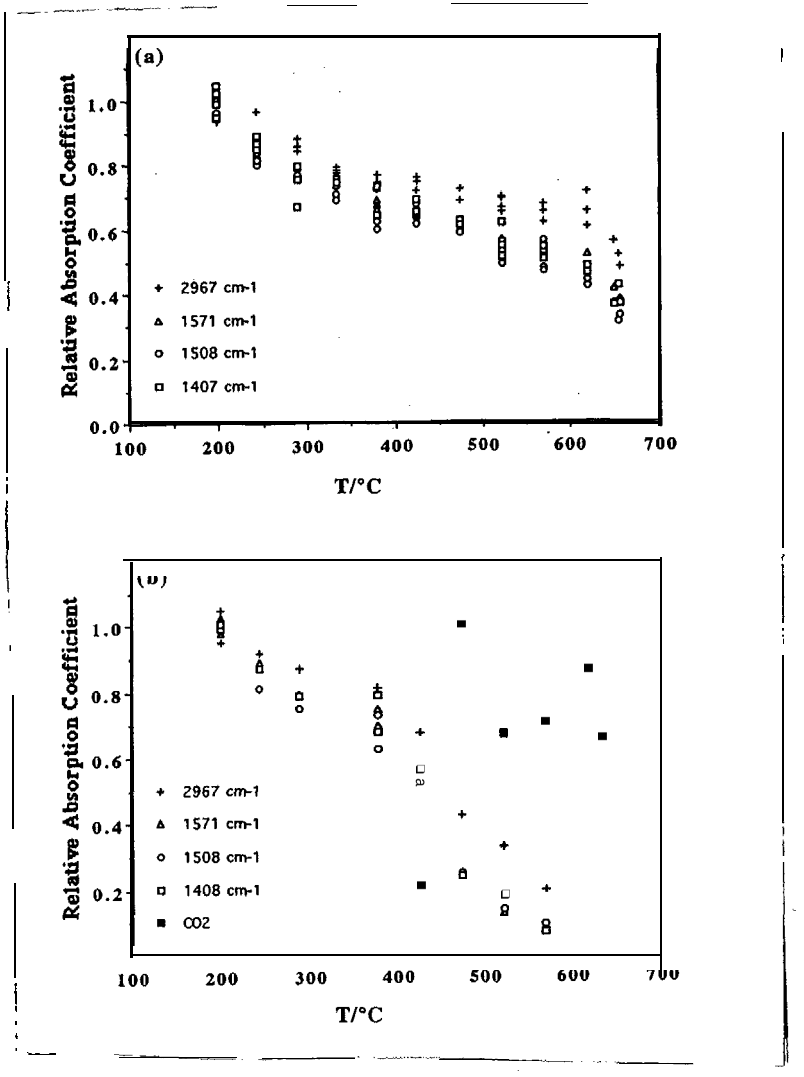

Figure 2: Plots of relative absorption coefficients as a function of temperature for $[Y(TMHD)_3]$ vapour under a total pressure of 1.33×10^3 Pa (10 torr) a without and (b) with oxygen

precursors which correspond very closely to those previously reported - Figure 3. Having struggled with this seemingly intractable problem for well over half the research programme it is now very satisfying that we have finally solved the problem and are able to get meaningful results. The technique has been applied to the study of the decomposition of the other precursors. This, coupled with the FTIR studies reported above, will allow valuable insights into the deposition chemistry of the individual elements and also mixtures of the elements.

3.2 *MOCVD of YBCO*

The optimised growth conditions for the deposition of $YBa_2Cu_3O_{7-\delta}$ on $SrTiO_3$ (100) are given in Table 1. Throughout the series of experiments carried out to obtain these conditions, the precursors were maintained at the elevated temperatures given in the Table. A batch of 20g was typically used for up to 8 weeks. Differential thermal analysis profiles of precursor material extracted from the pots after this time showed no signs of degradation. No anomalies in deposition or growth characteristics of the films were observed that could be associated with unusual precursor behaviour.

Initial concerns were to ensure sufficient water vapour was being directed to the reactor to convert all Ba deposit to the oxide. To this end, a slow carry over rate of the precursors was employed. Temperatures, pressures and flow rates through the precursor pots were chosen to give rise to adequate but not maximum growth rates. Deposition times of up to 200 minutes were employed to produce films of sufficient thickness (0.2 - 0.3 pm) which would enable reliable analysis to be carried out. As film quality improved, the carry over rate was gradually increased and the deposition time decreased accordingly so that the film thickness remained constant. Deposition rates increased from -0.08 to 0.14 μm h-*.

Table 2 shows typical EDX results for films deposited during the optimisation procedure. The first superconducting films deposited (e.g. Film #l) were black and had a mirror like surface. Closer inspection by SEM revealed a uniform grey background to the films that was interrupted by darker areas and brighter islands. This suggested the films were non-homogeneous at the micrometer level as has been reported previously [25]. EDX analysis over an area -500 μm x 350 μm yielded an average Y : Ba : Cu ratio of 1.32 : 2 : 4.28. Examination of the individual phases of the films (EDX resolution -2 μm) showed that the darker areas were rich in yttrium, the bright islands had a large excess of copper and the interconnecting matrix, with stoichiometry near 1:2:3, was the superconducting phase. Reduction in the partial pressures of Y and Cu in the gas phase (e.g. Films #2 to #6) resulted

Table 2 Film Characteristics for a MOCVD Superconducting $YBa_2C_{,}O_{7-\delta}$ Films

Run No	Averaged Y: Ba:Cu ratio (Area -500 x 350 μm[2)] (normalised to Ba)			Y: Ba:Cu ratio of HTS (Spot Analysis) (normalised to Ba)			Thick. of HTS Phase /μm (±0.03)	Growth rate /μm h-l	T_c /K (±0.5)	J_c at 77K /MA cm^{-2}
	Y (±0.03)	Ba	Cu (±0.09)	Y (±0.03)	Ba	Cu (±0.09)				
#1	1.32	2	**4.28**	1.03	2	2.93	0.28	**0.08**	93.2	0.90
#2	0.92	2	3.08	1.05	2	2.74	0.22	0.13	91.9	2.41
#3	1.02	2	3.43	1.11	2	2.81	0.21	0.13	91.0	3.28
#4	1.09	2	3.30	I .07	2	2.76	0.21	0.13	91.4	3.33
#5	1.04	2	2.91	1.09	2	2.81	0.23	0.14	91.3	5.33
#6	1.13	2	2.77	1.14	2	2.85	0.21	0.13	90.9	5.87

in the removal of the dark areas and a significant reduction in the number and dimensions of the Cu rich boulders whereas the concentration of the superconducting phase remained close to the desired 1:2:3.

X-ray diffraction was carried out to determine the orientation of the layer, Figure 4 shows a 2θ scan for a typical film, The scan shows substrate peaks and highly c-axis oriented $YBa_2Cu_3O_{7-\delta}$ peaks with very high intensities. The half maximum width of the $YBa_2Cu_3O_{7-\delta}$ (005) reflection was measured with rocking curve analysis. Figure 4 (inset) shows a Δω scan measured with the X-ray beam set at θ = 38.48°. FWHM for $YBa_2Cu_3O_{7-\delta}$ (005) was 0.216°. The results are indicative of epitaxial growth.

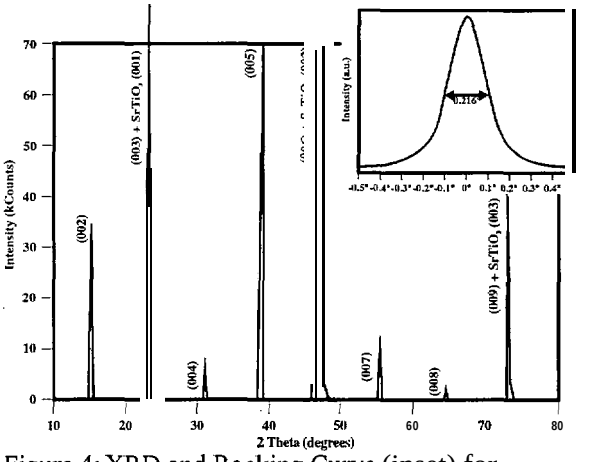

Figure 4: XRD and Rocking Curve (inset) for $YBa_2Cu_3O_{7-\delta}$ on $SrTiO_3$ (100)

AC susceptibility was used to investigate the superconducting properties of the film. Measurement of the temperature dependence of the ac susceptibility in a 0.1 Gauss excitation ac field, enabled the superconducting transition temperature, T_c, to be determined [26] (Table 2). Figure 5 shows a typical plot of ac susceptibility versus temperature. At 93.2 K, both the real and the imaginary part of the susceptibility start to deviate from their high temperature values which indicates the onset of superconductivity occurs at this temperature. The trough in the imaginary susceptibility curve at 92.9 K indicates that the Meissner effect is now strong enough to shield the excitation field at the centre of the film. Below 91.6 K the susceptibility values become constant which indicates that the excitation field is entirely screened by the superconducting film. As the stoichiometry of the films approached 1:2:3, T_c values fell towards 90 K. This was assigned to improved film formation and a probable hindrance towards 0_2 penetrating the film [27].

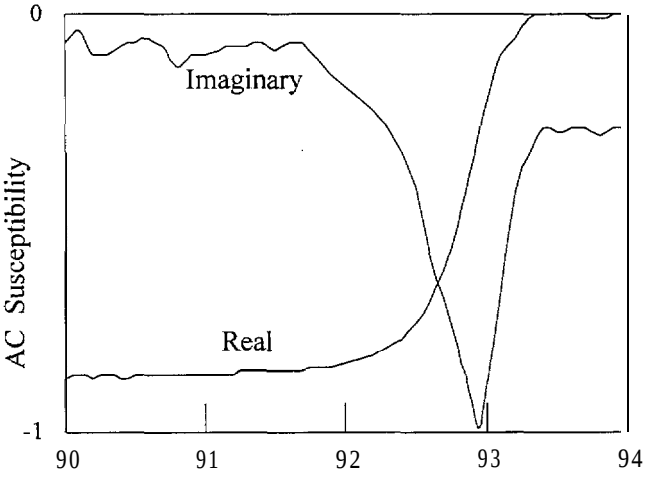

Figure 5: AC susceptibility plot for YBCO on $SrTiO_3$

In order to measure the critical current densities, $J_{c\ (inductive)}$, the AC susceptibility measurements were carried out using a 100 Gauss excitation field [23]. As sample morphology improved, $J_{c\ (inductive)}$ values at 77K increased from 0.9 to 5.9 MA cm^{-2} (Table 2). Two films were patterned to obtain transport current densities, $J_{c\ (transport)}$, for comparison with $J_{c\ (inductive)}$. The pattern for the transport measurement was a 0.6 mm long and 25 μm wide line connected with four contact pads. The patterning was carried out using electron beam lithography and Ar-ion milling. On the contact pads a thin layer of gold was deposited and patterned. During patterning of the gold layer, the films were reduced in thickness to ~0.16 pm. After patterning, the lines were found to be non superconducting owing to the out

diffusion of O_2 during ion milling. Superconductivity was restored by annealing in 0_2 (1 atm, 105 Pa) between 800 and 20 °C. Films annealed in this way can sustain further ion milling without losing their superconductivity. T_c for the patterned films was reduced to 89.0 and 89.5 K respectively. $J_{c\ (transport)}$ at 77 K could not be measured because the critical current was greater than that provided by the current source. At 88 K, $J_{c\ (transport)}$ values of 0.12 and 0.10 MA cm^{-2} were obtained. Smaller superconducting lines (0.1 mm x 2.5 pm) were then etched to enable $J_{c\ (transport)}$ at 77 K to be recorded. T_c was measured as 90.0 and 88.5 K and $J_{c\ (transport)}$ as 6.1 and 5.6 MA cm^{-2} respectively. T_c values could not be increased further by annealing.

Negative SIMS depth profiling was used to determine the concentration of fluorine in the films. The intensity of F^- and YO_2^- ions were monitored to a depth of up to 1pm for all samples. A standard was prepared by implanting fluorine into an $YBa_2Cu_3O_{7-\delta}$ film, deposited by laser ablation of a fluorine free target, with a dose of 1 x 10*^{4} F cm^{-2} at 180 keV. SIMS analysis of this implant standard yielded a relative sensitivity factor which was subsequently applied to directly convert F^-/YO_2^- ratios to fluorine concentrations. Dektak profilometry of the SIMS craters allowed depth calibrations to be made. To determine the effect of temperature on dopant species in one of the films, depth profiling was performed before and after annealing. The annealing process involved heating in N_2 (1 O mbar (10^3 Pa), 800 'C, 1 hour) and cooling in dry 0_2 to 300 "C (1 bar (10^5 Pa), 15 "C rei^n-').

The depth profile for fluorine in the film before and after annealing is shown in Figure 6. In both cases the fluorine concentration at the surface is initially very high but drops sharply to a level that remains constant throughout the bulk of the $YBa_2Cu_3O_{7-\delta}$ film. The concentration of fluorine in the $YBa_2Cu_3O_{7-\delta}$ layer before annealing was found to be higher than that detected after annealing. A sharp fall in concentration was observed for both profiles in the 0.25-0.30 μm region. This depth range is consistent with the film thickness determined by EDX and suggests a rapid fall in fluorine concentration occurs at the interface. The gradient of the decline is equal in both cases suggesting that annealing has not affected the interface. The difference in position of the two interfaces may be attributed to a difference in thickness of the film between the two areas analysed. The exact concentration of fluorine in the substrate cannot be accurately defined since the calibration was calculated relative to $YBa_2Cu_3O_{7-\delta}$ not $SrTi0_3$. Therefore, the fluorine concentrations in the $SrTi0_3$ are arbitrarily related to the concentrations in $YBa_2Cu_3O_{7-\delta}$ and, as such, are depicted as dotted lines in Figure 6.

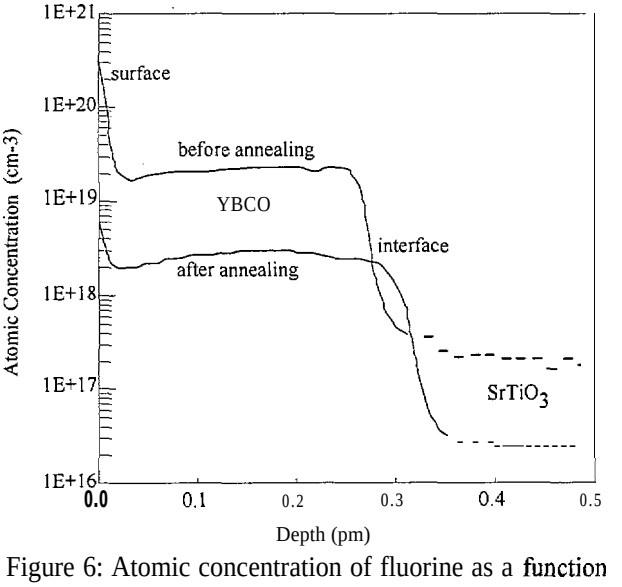

Figure 6: Atomic concentration of fluorine as a function of depth in YBCO (solid lines) on $SrTiO_3$ (broken lines) before and after annealing

Quantitative comparison with the fluorine implanted standard revealed that the untreated film contained -250 ppm F^- per $YBa_2Cu_3O_{7-\delta}$. This value decreased to -50 ppm upon annealing.

The loss of fluorine has been attributed to evaporation of fluorine out of the film. The uniform distribution of fluorine in the bulk of the film and the retention of the same concentration gradient at the interface excludes the possibility of migration of fluorine from the film to the substrate, A similar loss of fluorine upon annealing was observed by Hitchman *et al* [28] in fluorine doped polysilicon films.

The effect of low levels of fluorine remaining in an $YBa_2Cu_3O_{7-\delta}$ layer on device performance will need to be investigated. It is known [29] that traces of chlorine in semiconductor devices can lead to failure as a result of corrosion and there could be a similar problem in hybrid superconductor/semiconductor devices because of fluorine contamination in the $YBa_2Cu_3O_{7-\delta}$ layer. If the presence of fluorine does give rise to corrosion effects, either it will be necessary to try and remove the fluorine by complete hydrolysis or to find a suitable fluorine free barium precursor.

3.3 *MOCVD of $SrTiO_3$*

At the start of the experiments there were no process conditions known for the deposition of $SrTiO_3$. Only one article [30] was published using [Sr(HFA)$_2$.tetraglyme] and [Ba(HFA)$_2$.tetraglyme] in combination with [Ti(OPr^i)$_4$]. The process conditions in this article were used as a basis for the first series of experiments for the deposition of $SrTi0_3$ (see Table 3(a)).

Table 3 Process conditions for the deposition of $SrTiO_3$. - (a) without water; (b) with water

	a	b
Evaporator Temperature (°C)		
[Sr(HFA)$_2$.tetraglyme]	100	100
[Ti(OPr^i)$_4$]	20-40	-10
Carrier gas flow (seem)	33-83	83
Total gas flow (seem)	1667	1667
N_2:O_2	1:1	1:1
water flow (g/h)	0	5
Reactor pressure (mbar)	13.3	13.3
(Pa)	1350	1350
Susceptor Temperature (°C)	800	800

The results showed only deposition of $Ti0_2$ and SrO, both on Al_2O_3 (l-1 02) and Si (100). Although these two phases were grown with a 1:1 ratio, no $SrTi0_3$ was formed. It was observed that in order to get a Sr/Ti ratio of 1 in the deposited layer, a gas phase composition of-0.01 was required. Depositions using both the Sr and Ti precursors with O_2 but without H_2O resulted in oxide materials whereas, depositions using [Sr(HFA)$_2$.tetraglyme] and 0_2 gave SrF_2 as the main product. Only when using very low partial pressures of [Ti(OPr^i)$_4$], depositions using [Sr(HFA)$_2$.tetraglyme] and [Ti(OPr^i)$_4$] resulted in SrF_2 and TiO_2. It is believed that the iso-propoxide group acts as an *in situ* oxidiser of the SrF_2 just like water does in the deposition of YBCO from [Ba(HFA)$_2$.tetraglyme].

In contrast with the results in [30], $SrTi0_3$ was not deposited in any of the used growth conditions. Therefore a second set of experiments was performed using the addition of water. The optimised growth conditions can be found in Table 3(b). Oriented $SrTiO_3$ was found using a gas phase Sr/Ti ratio of 1. With these conditions, $SrTi0_3$ was successfully deposited on MgO (100) and YBCO (100).

X-ray diffraction (XRD) was carried out to determine the composition and orientation of the layers. The layers deposited on Si were found to be polycrystalline $SrTi0_3$ with some (1 11) orientation. Apart from a very tiny (1 11) peak only a axis oriented peaks were found for the

$SrTiO_3$ layer deposited on MgO (100). The quality of the $SrTiO_3$ layers deposited on laser ablated YBCO could not be determined by XRD because of overlapping peaks.

For the preparation of a YBCO/$SrTiO_3$/YBCO multilayer, a $SrTiO_3$ film was deposited on laser ablated YBCO (see section 3.4) during 35 minutes using the process conditions presented in Table 3(b). The resulting layer was grown with a deposition rate of 0.08 $mg/cm^2.hr$ and had an estimated thickness of 90nm.

3.4 *Multilayer*

Four point DC resistance measurements were carried out on the YBCO bridge on the top layer. The results showed that the top YBCO layer had a T_c of 89 K and a J_c of 2.7 x 10^6 A/cm^2 at 77K. The good quality of the YBCO layer below it was highly epitaxial. The resistivity of the $SrTi0_3$ layer was also characterised by measuring the resistance between the top and the bottom YBCO layers. At 300K the resistivity of the $SrTiO_3$ insulation layer was around 2 MΩcm and the resistivity increased as the temperature was decreased. The high resistivity revealed that there were no pin holes in the $SrTi0_3$ layer that may cause metallic contact between the top and the bottom YBCO layers.

4 Conclusions

High temperature superconducting thin films have been successfully deposited by MOCVD using the novel, fluorinated precursor [Ba(TDFND)$_2$.tetraglyme] which has been shown to be thermally stable for long periods at evaporation temperatures. Films deposited on $SrTi0_3$ (100) possessed critical temperatures -91K and critical current densities in excess of 5 MA cm^{-2}, The films have been grown epitaxially with c-axis orientation. Only residual fluorine levels were detected.

Multilayer deposition and patterning process has been developed based on laser ablated YBCO and $SrTi0_3$ layers. By applying the optimized process parameters highly sensitive magnetometers have been fabricated [24]. The multilayer patterning study applies the optimized multilayer patterning technique to the MOCVD layers. Test patterns have been prepared in a YBCO/$SrTiO_3$/YBCO structure where the $SrTiO_3$ dielectric layer was deposited on the YBCO bottom layer by MOCVD process. The electric properties of the test patterns have been characterized. The results show that highly epitaxial and insulating $SrTi0_3$ layers can been deposited on YBCO by MOCVD process. The resistivity of the $SrTiO_3$ layer is around 2 MΩ cm. The top YBCO layer has a T_c of 89 K and J_c of 2.7 MA/cm^2 at 77K.

5 Acknowledgements

We would like to thank the CEC for funding of BRITE/EURAM project No: BE-4020 Contract No: BREU 0438 and A Brown (Mats UK) for SIMS analysis.

6 References

[1] M. Leskelä, H. Mölsä and L. Niinisto, Supercond. Sci. Technol.,6 (1993) 627
[2] J. Zhao and P. Norris, Materials Science Forum, 130-132 (1993) 233
[3] T. Sugimoto, Materials Science Forum, 137-139 (1993) 395
[4] A.R. Barron and W.S. Rees, Adv. Mater. Opt. Electron., 2 (1993) 271
[5] H. Busch, A. Fink, A. Müller and K. Sarnwer, Supercond. Sci. Technol., 8 (1993) 42

[6] O. Thomas, J. Hudner, M. Östling, E. Mossang, B. Chenevier, F. Weiss, D. Boursier and J.P. Senateur, J. Alloys & Compounds, 195 (1993) 287
[7] E. Fitzer, H. Oetzmann, F. Schmaderer and G. Wahl, J. Physique, C2 (1991)713
[8] S.C. Thompson, D.J. Cole-Hamilton, D.D. Gilliland, M.L. Hitchman and J.C Barnes, Adv. Mater. Opt. Electron., 1 (1992) 81
[9] M.L. Hitchman, S.H. Shamlian, D.D. Gilliland, D.J. Cole-Hamilton, J.A.P. Nash, S.C. Thompson and S.L. Cook, J. Mater. Chem., 5 (1995)47
[10] K. Timmer, C. I.M.A. Spee, A. Mackor and H.A. Meinema, Eur. Pat. Appl. 405634 (1991) and J.A.T. Norman and G.P. Pez, J. Chem. Sot. Chem. Commun. (1991) 971.
[11] S.H. Shamlian, M.L. Hitchman, S.L. Cook and B.C. Richards, J. Mater. Chem., 4 (1994) 81
[12] J.A.P. Nash, J.C. Barnes, D.J. Cole-Hamilton, B.C. Richards, S.L. Cook and M.L. Hitchman, Adv. Mat. Opt. Electron. 5 (1995) 1
[13] A.Y. Kovalgin, F. Chabert-Rocabois, M.L. Hitchman, S.H. Shamlian and S.E. Alexandrov, J. De Physique IV, 5 (1995) C5-357
[14] K. Fröhlich, J. Souc, S. Chromik, D. Machajdik and V. Kliment, Physics C, 202 . (1992) 121
[15] I.M. Watson, M.P. Atwood, D.A. Cardwell and T.J. Cumberbatch, J. Mater. Chem., 4 (1994) 1393
[16] "Particle Beam Microanalysis - Fundamental Methods and Applications" E. Fuchs, H. Oppolzer and H. Rehme, VCH Weinheim (Germany) 1990
[17] B.C. Richards, S.L.Cook, D.L. Pinch and G. W. Andrews, J. de Physique IV,5(1995) C5-407
[18] A.F. Bykov, P.P. Semyannikov and K. Igumenov, *J. Thermal Anal., 38 (1992) 1463*
[19] A.F. Bykov, P.P. Semyannikov and K. Igumenov, *J. Thermal Anal., 38 (1992) 1477*
[20] Girolami G. S., Jeffries P.M. and Dubois L. H., J. *Am. Chem. Sot.,* 115 (1993) 1015
[21] S.C. Thompson, D.J. Cole-Hamilton, S.L. Cook and D. Barr, Eur. Pat. Appl. 92307390 (1993)
[22] K. Timmer, C. I.M.A. Spee, A. Mackor, H.A. Meinema, A.L. Spek and P. v/d Sluis, Inorg. Chimica Acts, 190 (1991) 109
[23] P. Vase, Y.Q. Shen and T. Freltoft, Physics C, 180 (1 99 1) 90
[24] Y. Q. Shen, Z. J. Sun, R. Kromann, T. Hoist, P. Vase and T. Freltoft, Appl. Phys. Lett. 67 (1995) 2081
[25] B. Schulte, M. Maul, P. Häussler, W. Becker, M. Schmelz, M. Steins and H. Adrian, J. Alloys& Compounds, 195 (1993) 299
[26] K.H. Müller, Physics C, 159(1989)717
[27] J.D. Jorgensen, B.W. Veal, A.P. Paulikas, L.J. Nowicki, G.W. Crabtree, H. Claus and W.K. Kwok, Phys Rev. B, 41 (1990) 1863
[28] M.L. Hitchman, J. Zhao, S.H. Shamlian, S. Affrossman, M. Hartshorne, E.A. Maydell and H. Kheyrandish, J. Mater. Chem., 4 (1994) 1835
[29] W.L. Bertram, "VLSI Technology" (Ed. S.M. Sze) McGraw Hill, New York (1983) Ch. 14
[30] B.W. Wessels, L.A. Wills, H.A. Lu, S.R. Gilbert, D.A. Neumayer, D.L. Schulz and T.J. Marks, Proc. 12th Int. Symp. on CVD (1993) 291

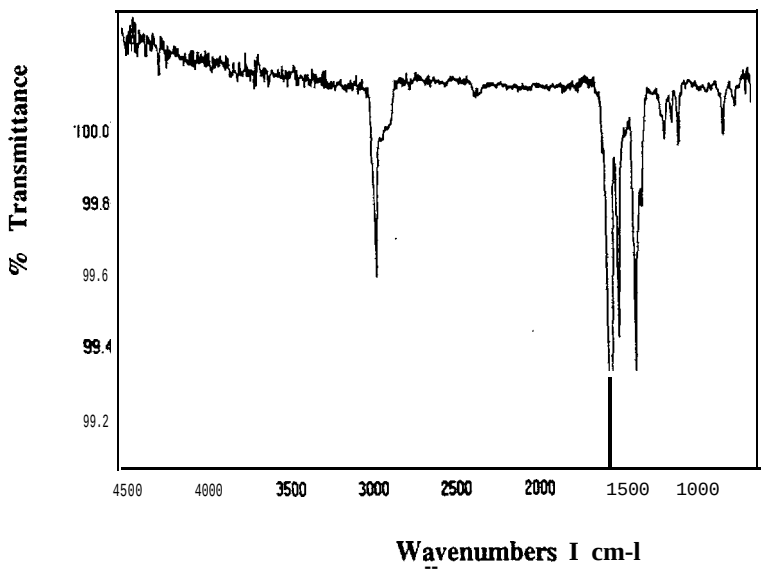
% Transmittance
100.0
99.8
99.6
99.4
99.2
4500
4000
3500
3000
2500
2000
1500
1000
Wavenumbers I cm-l

BE4020

Fg 1.

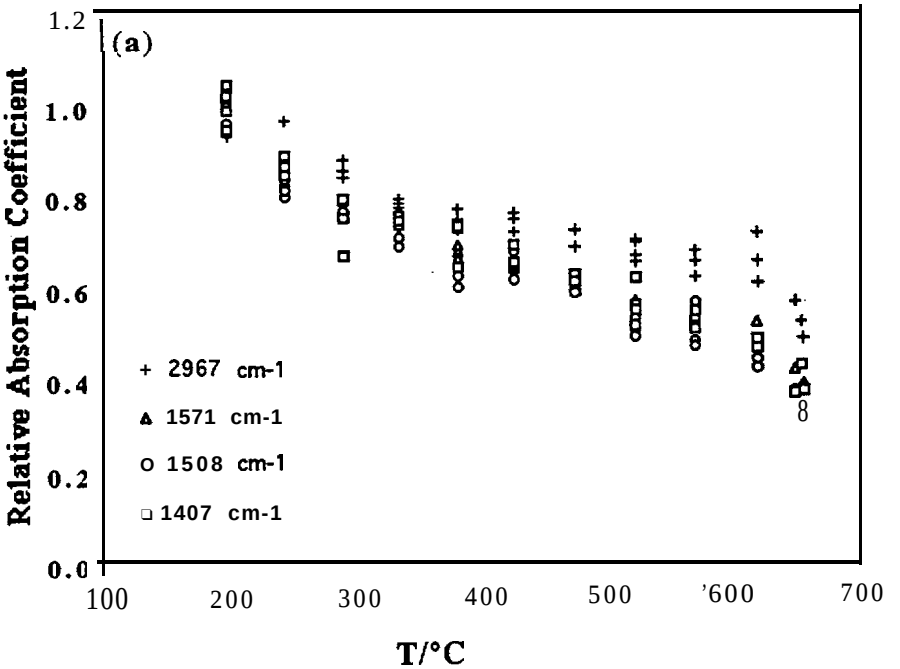
(a)
Relative Absorption Coefficient
1.2
1.0
0.8
0.6
0.4
0.2
0.0
+ 2967 cm-1
▲ 1571 cm-1
O 1508 cm-1
□ 1407 cm-1
100
200
300
400
500
'600
700
T/°C

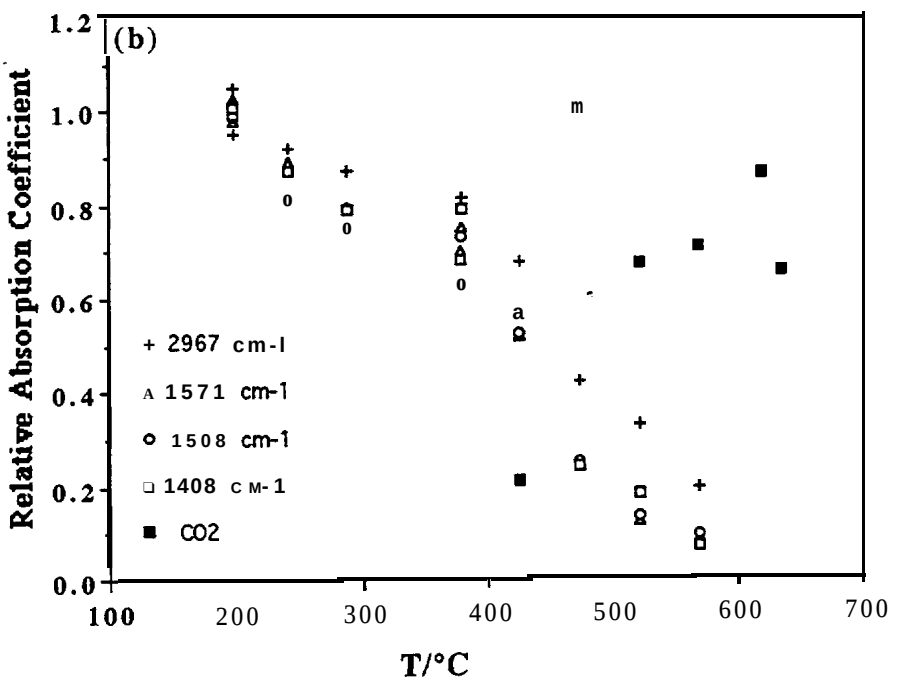
(b)
Relative Absorption Coefficient
1.2
1.0
0.8
0.6
0.4
0.2
0.0
+ 2967 cm-1
▲ 1571 cm-1
O 1508 cm-1
□ 1408 CM-1
■ CO2
100
200
300
400
500
600
700
T/°C

BE4020
Fig 2

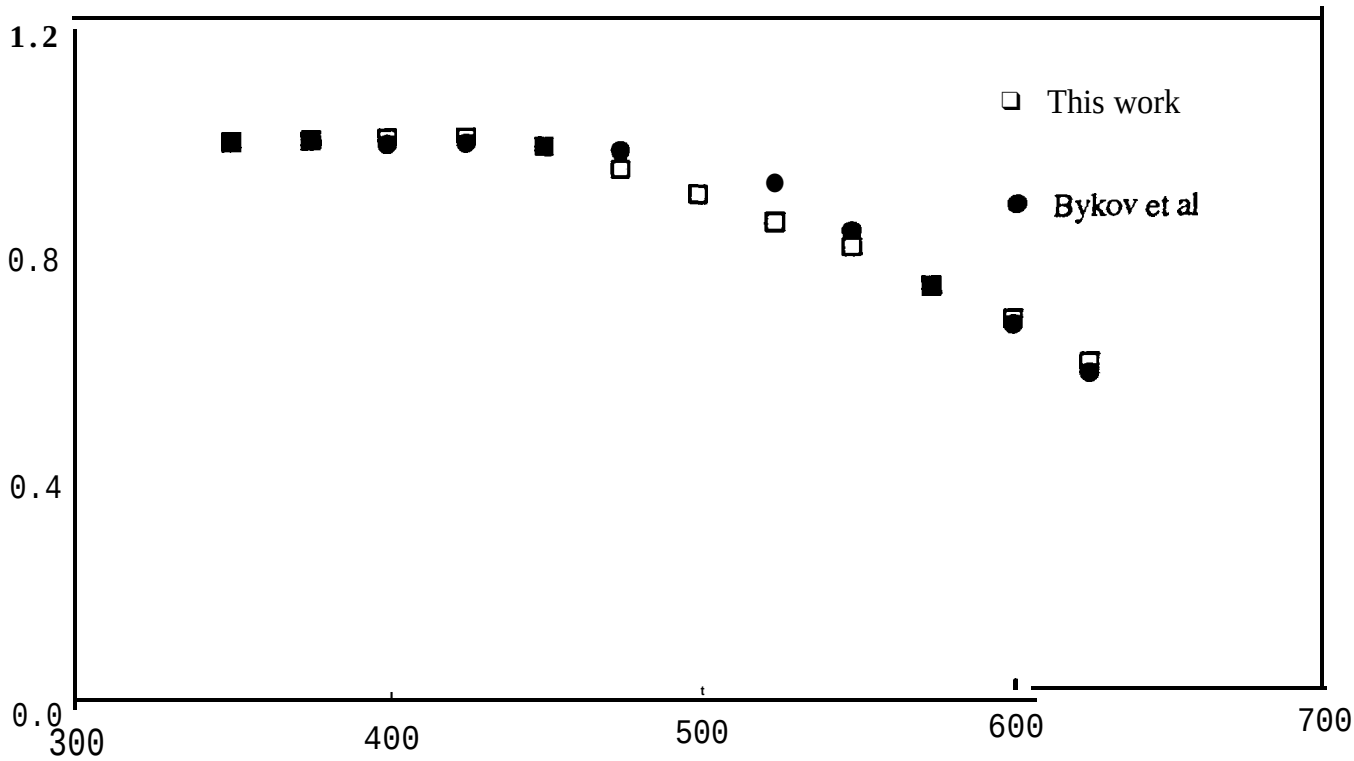

Normalised Intensity

Decomposition Temperature /C

Fig 3

BE4020